

## Spatial distribution of the magnetic disturbances at European midlatitudes during substorms: case study

---

V. Guineva<sup>a</sup>, R. Werner<sup>a</sup>, R. Bojilova<sup>b</sup>, A. Atanassov<sup>a</sup>, L. Raykova<sup>a</sup> and D. Valev<sup>a</sup>

*aSpace Research and Technology Institute (SRTI), Bulgarian Academy of Sciences, Stara Zagora Department,*

*P.O.Box 73, 6000 Stara Zagora, Bulgaria*

*bNational Institute of Geophysics, Geodesy and Geography (NIGGG), Bulgarian Academy of Sciences, bl.3 „Acad. G.Bonchev“ str., 1113 Sofia, Bulgaria*

*E-mail: [v\\_guineva@yahoo.com](mailto:v_guineva@yahoo.com), [rolwer52@yahoo.co.uk](mailto:rolwer52@yahoo.co.uk), [rbojilova@geophys.bas.bg](mailto:rbojilova@geophys.bas.bg), [at\\_m\\_atanassov@yahoo.com](mailto:at_m_atanassov@yahoo.com), [heiti456@gmail.com](mailto:heiti456@gmail.com), [valev@gbg.bg](mailto:valev@gbg.bg)*

This work is aimed to study the spatial distribution of the magnetic field components variations during substorms. In this purpose, an isolated substorm, the substorm on 22 March 2013 at ~23:10 UT, with central meridian over Europe has been chosen. Magnetic field data from INTERMAGNET, SuperMAG and IMAGE databases have been used. The X and Y variations due to the substorm were computed for more than 40 stations based on the developed programs. Maps of the spatial distribution of the magnetic variations have been created, longitudinal and latitudinal profiles for this event have been constructed for the time of the midlatitude positive bay (MPB) maximum at Panagjurishte (PAG) and some other moments of the substorm development. Some characteristics as the line of sign conversion latitude, the central meridian, the longitudinal and latitudinal extent of the positive bays and the latitudinal and longitudinal dependence of the variations have been estimated.

*11th International Conference of the Balkan Physical Union (BPU11),  
28 August - 1 September 2022  
Belgrade, Serbia*

## 1. Introduction

Magnetospheric substorms are related to a number of processes in the magnetosphere and ionosphere, generalized by Akasofu [1]. One of them are the specific disturbances of the magnetic field on the Earth surface. During substorms, characteristic negative bays in the X magnetic component occur, usually at auroral latitudes ( $60^{\circ}$ - $70^{\circ}$  MLAT) [2], but depending on the interplanetary and geomagnetic conditions also at high latitudes ( $>70^{\circ}$  MLAT) [3, 4, 5] and lower latitudes (to  $\sim 50^{\circ}$  MLAT) [6]. And vice versa, at midlatitudes, weak disturbances related to substorms can be observed at the Earth surface representing positive bays in the X component [7]. According to modern understanding, the behavior of the Earth's surface magnetic field during magnetospheric substorms is the result of the formation of a current system called the substorm current wedge [7, 8]. The negative bays in the X component are driven by the westward electrojet, and the positive bays at midlatitudes, are associated with the field aligned currents. The behavior of the magnetic field at midlatitudes can be used to study the magnetospheric substorms. For instance, the onset of the midlatitude positive bays (MPB) is a good indicator of the beginning of the substorm expansion phase (e.g. [9, 10]). By the Y component of the magnetic field at midlatitudes the substorm meridian [11, 12] and the direction of the field aligned currents [13] were determined. Different spatial or temporal distributions of the magnetic perturbations at midlatitudes have been used to determine some substorm parameters [e.g. 14, 15].

In this work the spatial and temporal development of the magnetic field perturbations at midlatitudes due to substorms has been examined based on maps of the spatial distribution and latitudinal and longitudinal profiles of the magnetic perturbations on the Earth surface at chosen typical times. An isolated substorm in non-storm conditions, the substorm on 22 March 2013 at about 23:10 UT with central meridian over Europe has been singled out for the study.

## 2. Data used

To verify the interplanetary and geomagnetic conditions, data for the Interplanetary Magnetic Field (IMF) and the solar wind parameters from the OMNI database have been used.

The magnetic field components from different magnetic stations have been derived from the databases INTERMAGNET, SuperMAG, and IMAGE.

We tried to find isolated substorms (no strong magnetic disturbances at least 3 hours before the considered substorm), which developed over Europe (the central meridian of the substorm located near Middle Europe) during comparatively quiet geomagnetic conditions and without a geomagnetic storm in progress.

Two such events satisfying the above conditions, namely the substorm on 22 March 2013 at  $\sim 23:12$  UT and the one on 11 May 2015 at  $\sim 22:49$  UT, have been examined. The results for the substorm on 22 March 2013 are presented in detail in this paper.

Data from 53 European stations at auroral and midlatitudes and from 6 midlatitude Asian stations have been used for the study of the magnetic disturbances due to the substorm under consideration. The following stations have been included in the study: BDV, BEL, BOX, BRZ, CLF, DUR, EBR, ESK, FUR, GUI, HAD, HLP, HRB, IZN, KIV, KRT, LER, LVV, MNK, MOS, NGK, NUR, OUJ, PAG, PEG, SFS, SPT, SUA, SUW, THY, UPS, VAL, WNG, ABK, BJN, DOB, HAN, HOP, IVA, JCK, KAR, KEV, LYC, LOZ, MAB, MEK, MUO, NOR, PEL, RVK, SOL,

TRO, SOR, ARS, NVS, IRT, CNH, YAK, MGD. In Fig.1 the locations of the European stations used in this study with the station names abbreviations nearby are given.

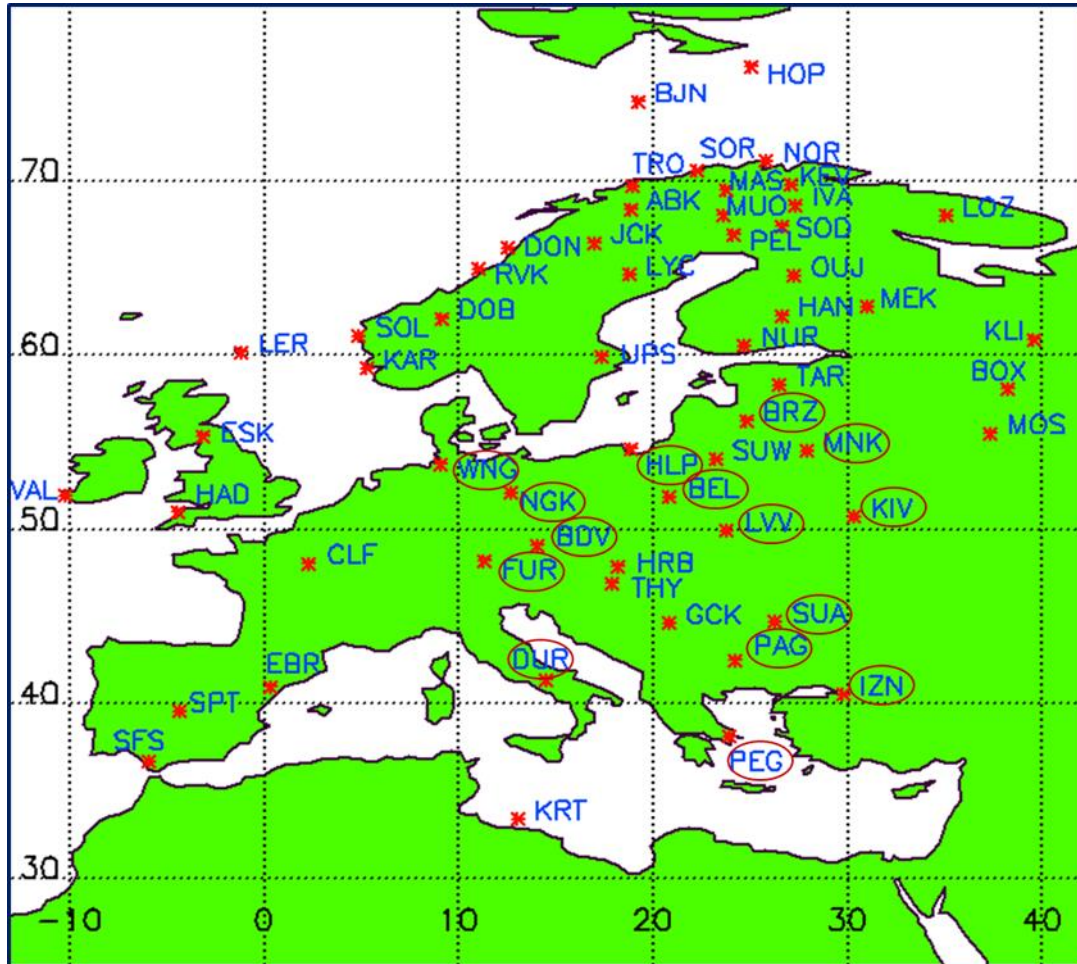


Fig.1. Locations of the European magnetic stations (asterisks) with the name abbreviations. The names of the stations, data from which are used to compute the European MPB index are surrounded by ellipses.

### 3. Interplanetary and geomagnetic conditions

The interplanetary and geomagnetic conditions during which the substorm on 22 March 2013 originated are given in Fig.2. From up to down, the following quantities are presented: the magnitude of the IMF vector  $B$ , the  $B_y$  and  $B_z$  components of the IMF, the flow speed  $V$ , the proton density  $N$ , the temperature  $T$ , the flow pressure  $P$ , the AL index and the SYM/H index. The left panel covers the time interval from 12 UT on 21 March 2013 to 06 UT on 23 March 2013, and the right one – from 21:30 UT on 22 March 2013 to 01:30 UT on 23 March 2013. The time of the substorm onset is marked by a vertical line in both panels. From Fig.2 it is seen that the conditions are quiet, in the two hours preceding the substorm,  $B$  is in the range  $2 \div 4$  nT,  $B_y$  is negative, about  $-2.5$  nT,  $B_z$  is negative for more than 1 hour before the substorm, in the range  $-2 \div -3$  nT. The values of  $V$ ,  $N$ ,  $T$ , and  $P$  are low, in the range  $375\text{-}395$  km/s,  $3.5 - 4.5$  n/cc,  $4 \div 5.5 \cdot 10^4$  K, and  $1 - 1.5$  nP, respectively. However, at the substorm beginning, small, but sharp jumps in these quantities are observed, of about  $20$  km/s,  $1$  n/cc,  $0.7 \cdot 10^4$  K, and  $0.5$  nP (right

panel of Fig.2). The SYM/H index is about  $-22$  nT, and even if it is decreasing, it doesn't surpass  $-27$  nT, testifying that there is no a geomagnetic storm at this time. The minimum in the AL index, related to the examined substorm, is about  $-300$  nT. The IL index, computed for the PPN-NAL chain of the IMAGE stations, which is connected to the development of substorms over Europe (not presented here), reaches about  $-350$  nT.

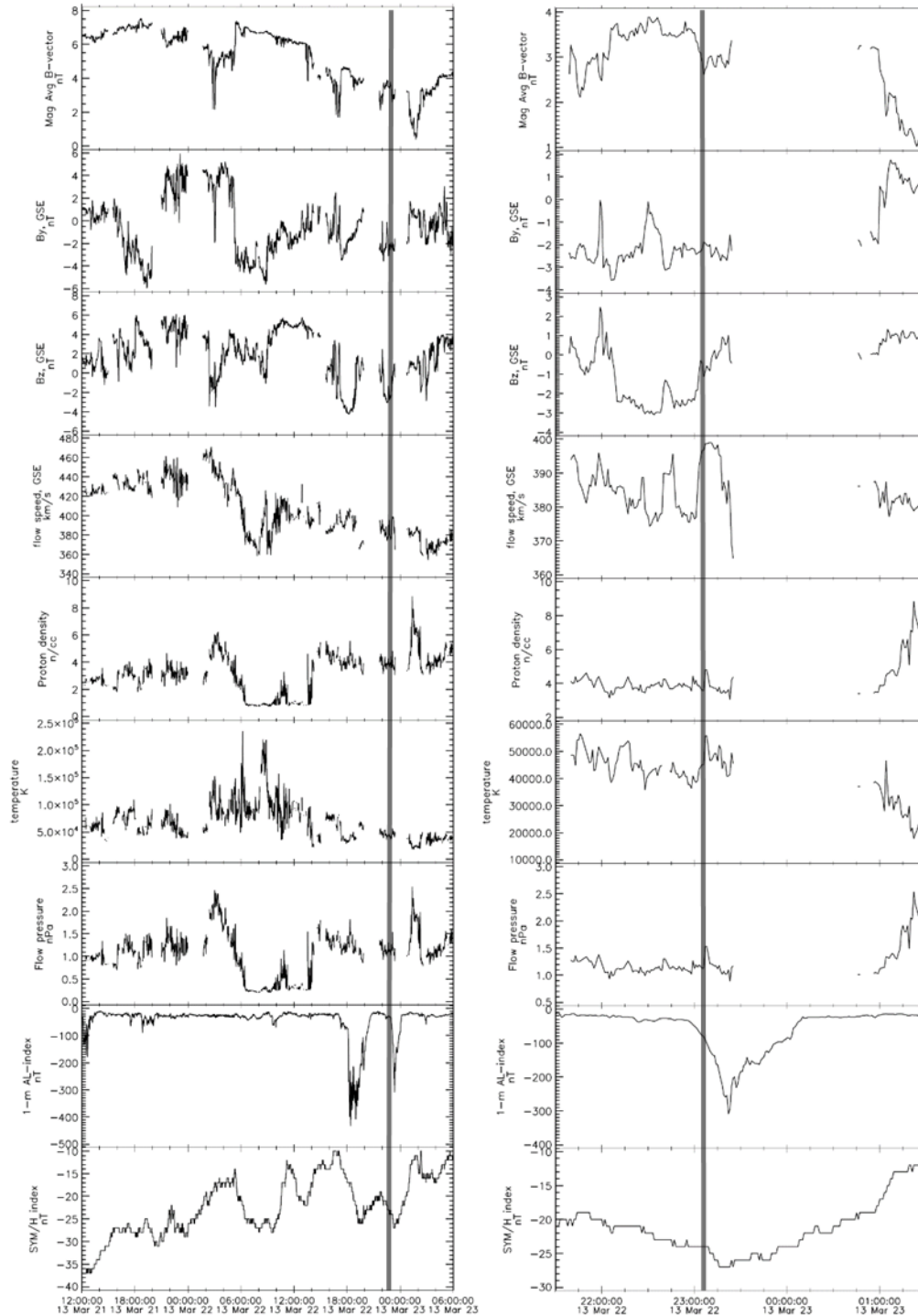


Fig.2. Interplanetary and geomagnetic conditions from 12 UT on 21 March 2013 to 06 UT on 23 March 2013 (left panel) and from 21:30 UT on 22 March 2013 to 01:30 UT on 23 March 2013 (right panel). The straight vertical lines indicate the time of the substorm onset.

#### 4. Processed magnetic field disturbances

To obtain the magnetic variations at the earth surface, provoked by the substorm, the created processing method described in [16, 17], based on the algorithm by McPherron and Chu [10] and some new developments, has been applied on the raw magnetic field data for the stations, enumerated in the section “Data used”. The basic steps of this method are: construction of a long array of 36000 data points spaced in minutes for an interval of 25 days, centered on the day of the substorm under consideration; preprocessing, including gaps and peaks detection and removal; estimation and subtraction of the main field; removing of the very disturbed days (outliers) by Grubbs test; determination and subtraction of the mean solar quiet day (Sq) variations; high-pass filtration of the obtained X and Y component variations; computing of the horizontal power. The obtained variations of the X, Y components and the horizontal power have been used to examine the behavior of the magnetic field in a large area during the specified substorm event. In Fig.3, the variations of the X component of the magnetic field at chosen stations from 20 UT to 24 UT on 22 March 2013 are shown: a) X component by the PPN-NAL latitudinal chain of the IMAGE network. The ellipse indicates the substorm disturbances; b) X variations computed by our method for some stations from the PPN-NAL chain. The geomagnetic latitude decreases from up to down in the figure panels; c) obtained X variations at lower latitudes stations located near the PPN-NAL meridian; d) X variations at stations, located at different geomagnetic longitude and at near geomagnetic latitudes. The X series are arranged from up to down by the station locations from East to West, i.e. by decreasing geomagnetic longitudes. The vertical lines in panels b), c) and d) indicate three typical times of the substorm development, 23:16 UT, 23:27 UT and 23:40 UT, at which X had a maximum at different stations. For these times, maps and latitudinal and longitudinal profiles of the X and Y perturbations have been constructed.

#### 5. Maps of the X and Y perturbations

In Fig.4 and Fig.5, the computed maps at the three moments, listed above, of the X and Y perturbations are presented, respectively. The maps of the X and Y distributions are plotted on the geographic grid, with continental boundaries traced out. The stations locations are marked by asterisks, and nearby the station names abbreviations are written. The distribution of X variations is restored to optimal limits over a maximally large range of latitudes, and the X distribution maps are from 38° to 73° LAT and from 10° to 32° LON. Accordingly, the Y variations are calculated over a maximally large range of longitudes, and the Y distribution maps are from 38° to 55° LAT and from -10° to 35° LON. This allows to better follow the development of the X variations depending on the latitude and of the Y variations depending on the longitude. Between the negative bays at auroral latitudes and the positive bays at midlatitudes, a boundary of the transition from negative to positive values, or the boundary of the midlatitude positive bays (MPB) presence to the North, is observed. In Fig.4, this boundary is clearly outlined across the entire width of the maps. At 23:16 UT and 23:27 UT the transition from negative to positive X perturbations is near the LYC and OUI stations, i.e. about 64°-65° LAT (~61° MLAT) (the left and central panels of Fig.4), and at 23:40 UT this boundary is replaced near the ABK, MUO, SOD stations, i.e. about 67°-68°LAT (~64°-65° MLAT) (the right panel of Fig.4).

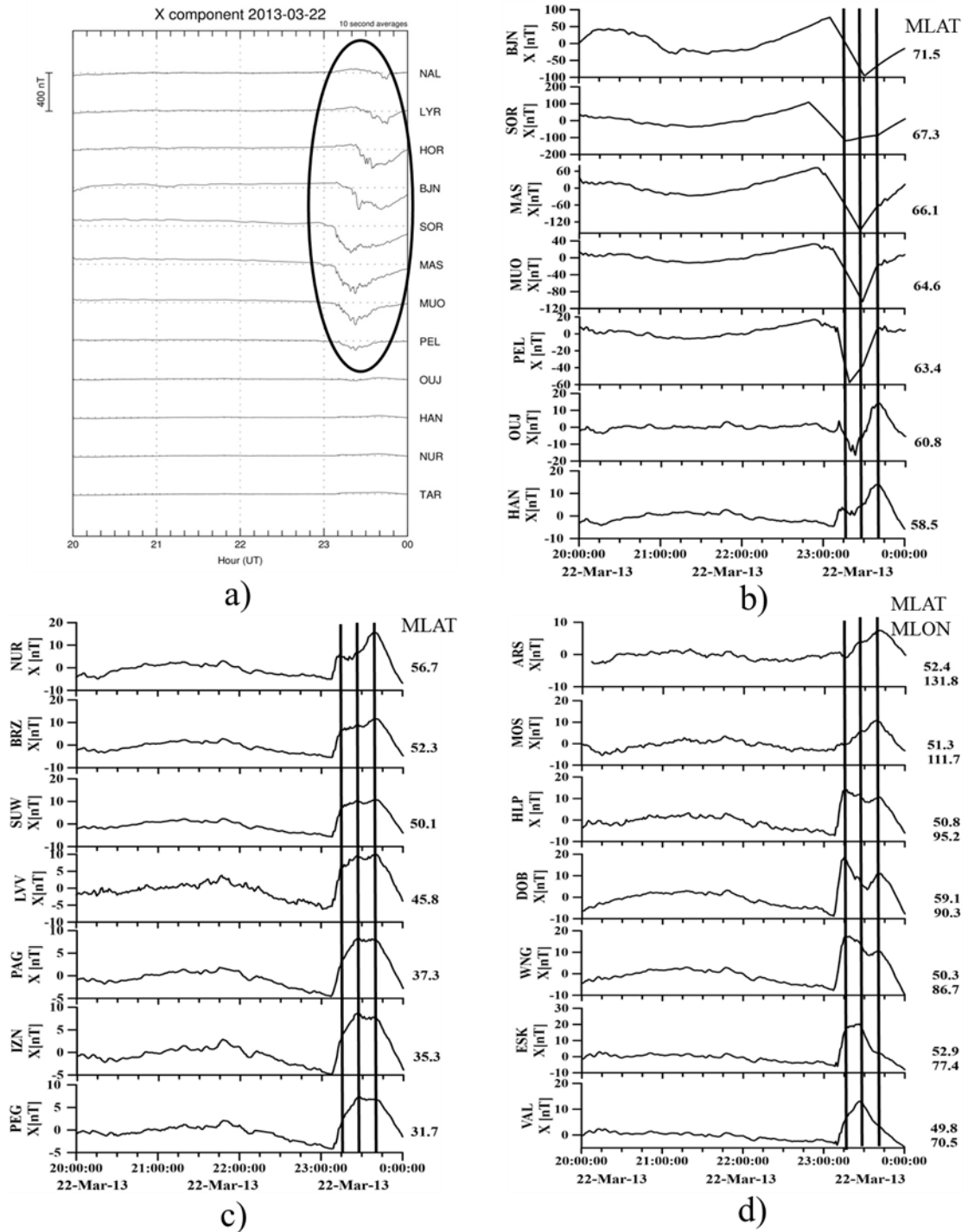


Fig.3. Magnetic field variations from 20 UT to 24 UT on 22 March 2013 at different stations: a) the PPN-NAL chain magnetic field, given by the IMAGE database. The ellipse marks the substorm disturbances; b) X variations computed by our method for some stations from the PPN-NAL chain; c) X variations for stations at lower latitudes; d) X variations for stations at different geomagnetic longitudes and at near geomagnetic latitudes. The X series are arranged from up to down by the station locations from East to West, i.e. by decreasing geomagnetic longitudes. The vertical lines in panels b), c) and d) indicate three typical times of the substorm development, 23:16 UT, 23:27 UT and 23:40 UT, at which X had a maximum at different stations.



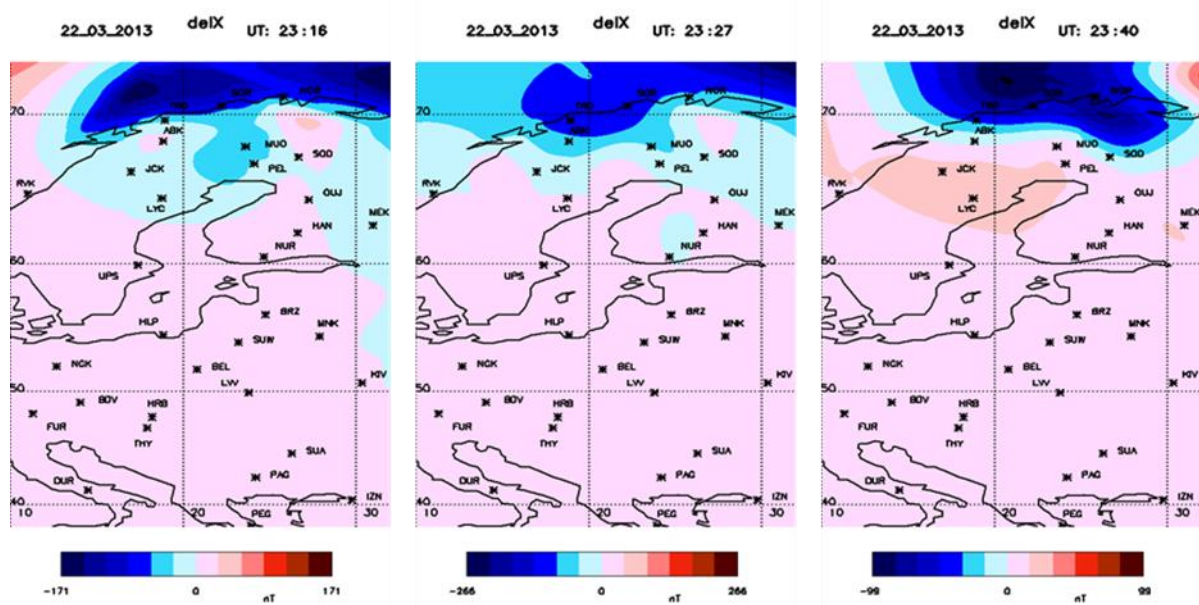


Fig.4. Maps of the X variations distributions in the range  $38^{\circ}$  -  $73^{\circ}$  LAT and  $10^{\circ}$  -  $32^{\circ}$  LON at 23:16 UT (left panel), 23:27 UT (middle panel) and 23:40 UT (right panel).

The Y perturbations distribution gives information about the location of the central meridian of the substorm. It coincides with the longitude of passage of the Y perturbations through zero [16, 17]. From the upper and middle panels of Fig.5, at 23:16 UT and 23:27 UT, it is seen that the substorm meridian in middle Europe is near the FUR and DUR stations, i.e. about  $11^{\circ}$ - $14^{\circ}$  LON ( $\sim 84^{\circ}$  MLON). The Y perturbations distribution at 23:40 UT (lower panel of Fig.5) shows that the substorm meridian moved to the East and it was near but outside the map boundary of  $35^{\circ}$  LON.

## 6. Perturbations profiles

As it is seen from Fig.4 and Fig.5, the examined boundaries are not at the same latitude or longitude, but they form curves which depend on the longitude or latitude. By reason of this, Europe and part of Asia are divided in narrower latitudinal and longitudinal bands, and profiles of the X and Y perturbations have been constructed to study their spatial and temporal development. The latitudinal profiles are examined in the following intervals of geomagnetic longitude:  $60^{\circ}$ - $80^{\circ}$ ,  $80^{\circ}$ - $95^{\circ}$ ,  $95^{\circ}$ - $100^{\circ}$ ,  $100^{\circ}$ - $105^{\circ}$ ,  $105^{\circ}$ - $115^{\circ}$ . For the longitudinal profiles, the following bands of geomagnetic latitudes are used:  $14^{\circ}$ - $30^{\circ}$ ,  $30^{\circ}$ - $40^{\circ}$ ,  $40^{\circ}$ - $50^{\circ}$ ,  $50^{\circ}$ - $55^{\circ}$ ,  $55^{\circ}$ - $60^{\circ}$ . The obtained profiles are shown in Fig.6. The left column of panels presents the profiles at 23:16 UT, the middle column – the profiles at 23:27 UT, and the right panels – the profiles at 23:40 UT. In the upper and middle rows, the latitudinal and longitudinal profiles of the X perturbations are shown, respectively. The vertical blue lines indicate the latitudinal and longitudinal extent of the midlatitude positive bays (MPB) at the limit of 5 nT, and the black ones – at the limit of 0 nT. We consider a perturbation of the X component to be significant if it is greater than or equal to 5 nT, that is why the extent of MPB is estimated by the 5 nT limit. The bottom row presents the longitudinal profiles of the Y perturbations. The red vertical lines denote the location of the central meridian of the substorm (where Y crosses the zero line).



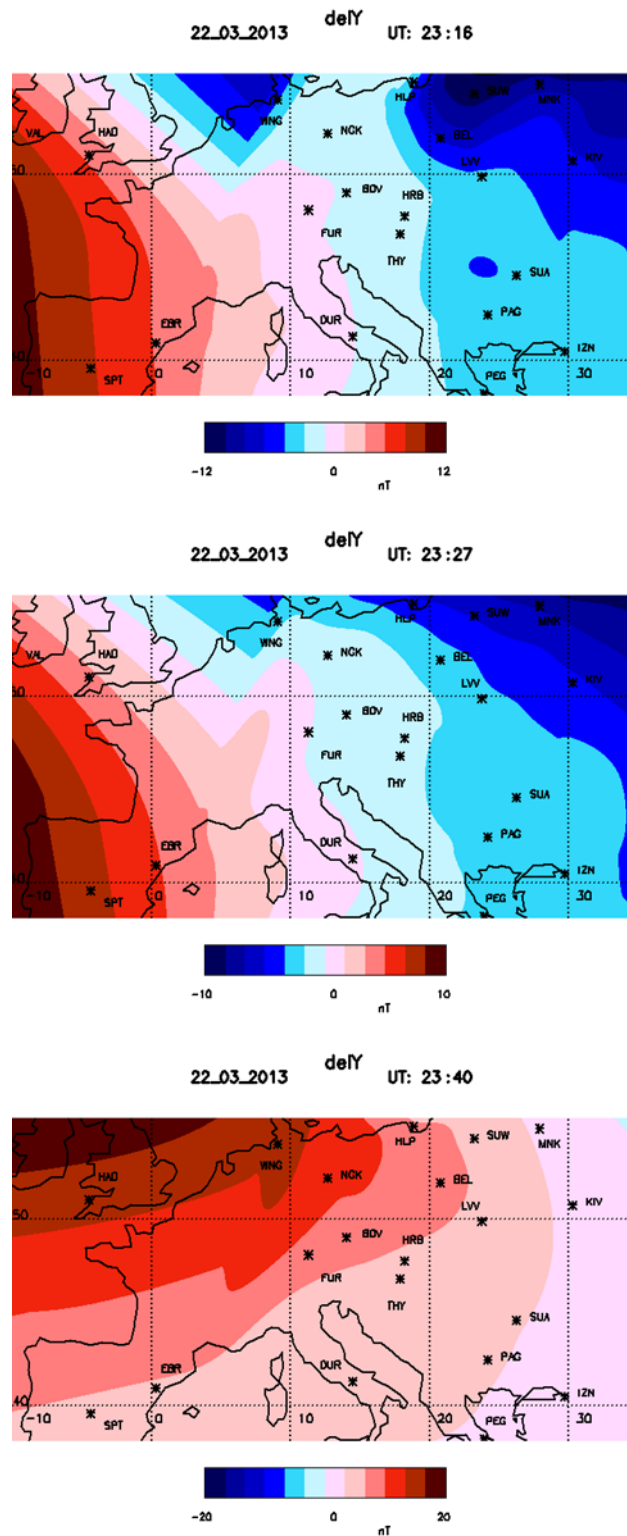


Fig.5. Maps of the Y component distributions in the range  $38^{\circ} \div 55^{\circ}$  LAT and  $-10^{\circ} \div 35^{\circ}$  LON at 23:16 UT (upper panel), 23:27 UT (middle panel) and 23:40 UT (bottom panel).

The results from the profiles are summarized in Table 1. The row “MLAT limits” gives the range of presence of MPB by geomagnetic latitudes, “Sign conv.” is the sign conversion

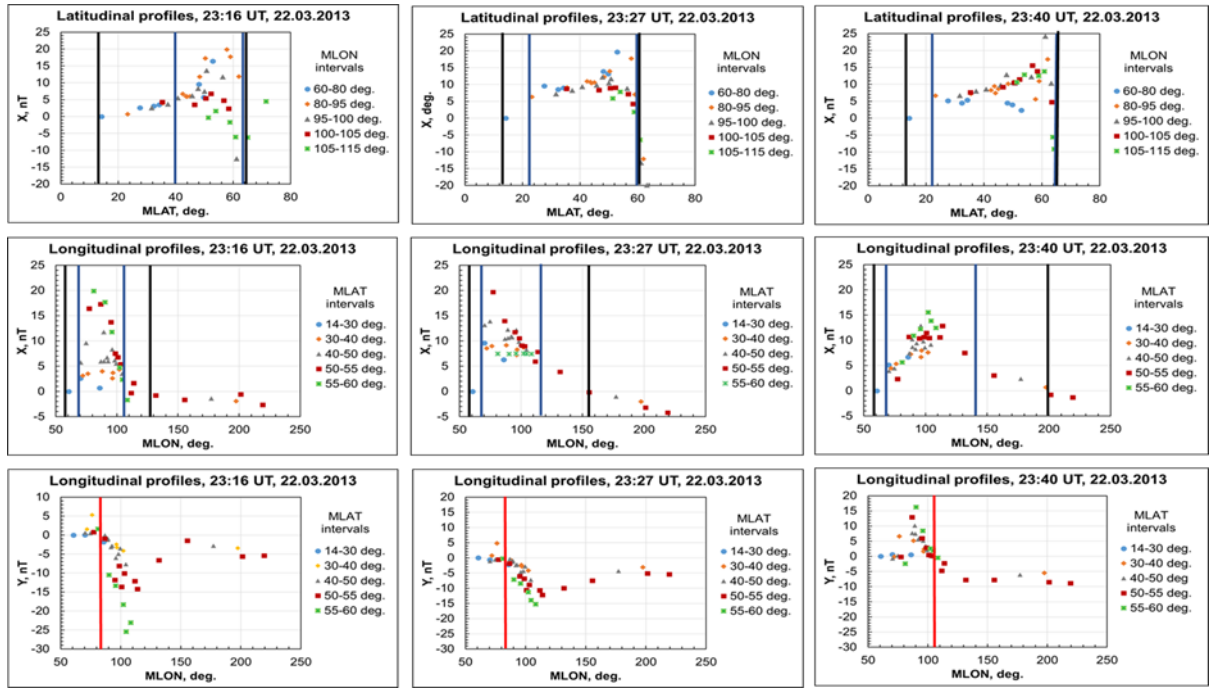


Fig.6. Latitudinal profiles of the X perturbations (upper row) and longitudinal profiles of the X and Y perturbations (middle and bottom rows) at 23:16 UT (left column), 23:27 UT (middle column) and 23:40 UT (right column).

Table 1. Midlatitude positive bays extent and some characteristics.

UT:	23:16	23:27	23:40
MLAT limits	~40°-65°	~23°-60°	~23°-63°
Sign conv.	67°	60°	63°
Max at MLAT	58°(51°-59°)	53°(53°-58°)	61°(56°-62°)
Lat. extent	~25°	~37°	~40°
MLON limits	~70°-104°	~70°-120°	~70°-140°
Max at MLON	~82°	~82°	~102°
Long. extent	~34°	~50°	~70°
$Y_0$	~84°	~84°	~106°

geomagnetic latitude, “Max at MLAT” is the geomagnetic latitude, at which the maximal X perturbation is observed, “Lat. extent” is the latitudinal extent of the positive bays, “MLON limits” is the range of presence of MPB by geomagnetic longitudes, “Max at MLON” is the geomagnetic longitude, at which the maximal X perturbation is observed, “Long. extent” is the

longitudinal extent of the positive bays, “ $Y_0$ ” is the geomagnetic longitude at which  $Y$  crosses the zero line (substorm meridian).

The obtained latitudinal dependence of the  $X$  variations is as follows: after the sign conversion latitude  $X$  increases, reaches a maximum close to it, and decreases gradually (the upper panel of Fig.6). This confirms our previous results about the behavior of the MPB after the sign conversion latitude [16, 17]. Besides, the maximal value of  $X$  variations is located at different latitude for the different longitudinal intervals.

The sign conversion latitude is in the range  $60^\circ$ - $67^\circ$ MLAT.

In longitudinal direction, the maximal variations are observed near the crossing of the zero line by  $Y$ . This result confirms that the central meridian of the substorm can be determined by both: crossing of zero line by the  $Y$  component and maximal values of the  $X$  component in longitudinal direction.

The latitudinal and longitudinal extent increase during the substorm development.

## 7. MPB index

The European MPB index was obtained by averaging the horizontal power of the magnetic field at 16 stations located in Middle Europe. Stations distributed comparatively uniformly over Middle Europe have been chosen. In fig.1, presenting the European magnetic stations locations, the abbreviations of the names of the stations used for the MPB index computing are indicated by ellipses around them. The MPB index on 22 March 2013, obtained by that means, is drawn in Fig.7.

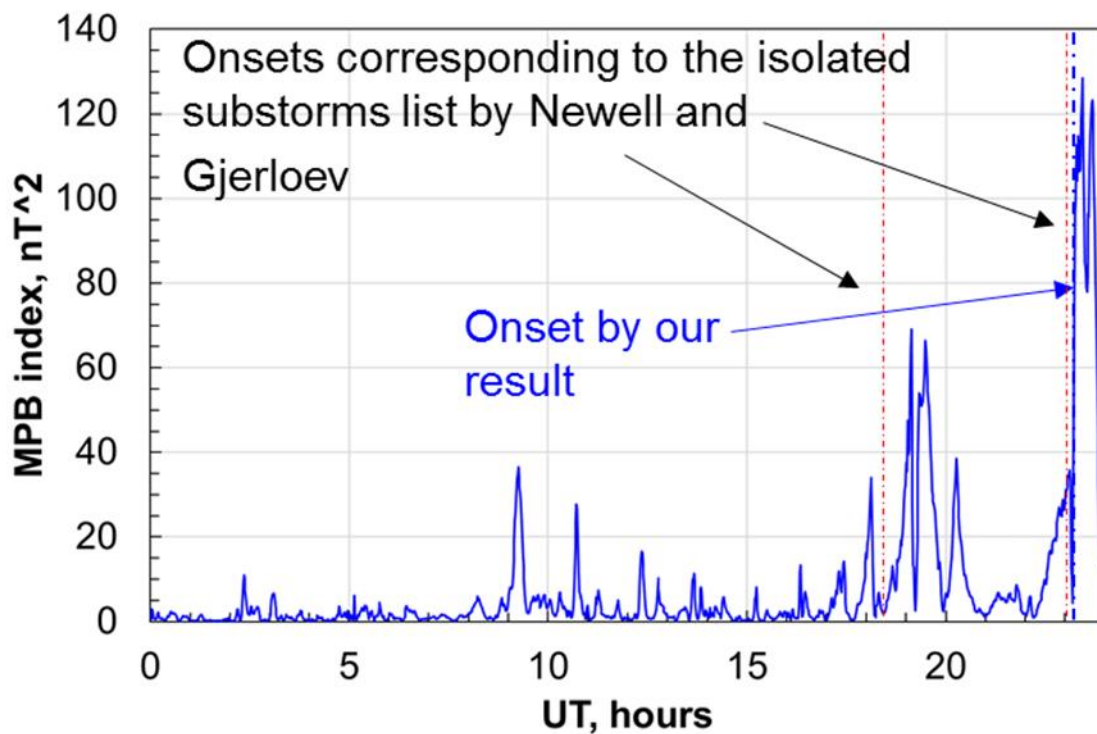


Fig.7. European MPB index on 22 March 2013. The substorm onset determined by our results and the onsets, given by Newell and Gjerloev [20] are indicated by vertical dashed-dotted lines and by arrows.

The onset of the examined substorm, determined by the peak minimum before the MPB maximum associated with the substorm, is indicated. In Fig.6 the substorm onsets by Newell and Gjerloev [20] based on the SML index, are given, as well. It is seen, that the onset determined in this work, and the one by Newell and Gjerloev for the same substorm, are very close to each other. We compared also the MPB index, obtained here, with the one given by Chu [21]. We obtained a MPB maximum of 126.83 nT<sup>2</sup>, against a maximum of 113.77 nT<sup>2</sup>, which shows a very good coincidence of both results and testifies that our results are accurate.

## 8. Summary and conclusions

The development of an isolated expanded substorm under quiet, non-storm conditions, begun at ~23:10 UT on 22.03.2013 is presented in detail. Data from 59 magnetic stations were processed. Maps of the X magnetic component in the range 38°÷73° geographic latitude, 10°÷32° geographic longitude, and of the Y component in the range 38°÷55° geographic latitude, -10°÷35° geographic longitude for 3 moments of the substorm development: 23:16 UT, 23:27 UT and 23:40 UT, when maxima were observed at different stations, have been constructed. Latitudinal and longitudinal profiles for the same 3 moments were built up as well.

By the use of the maps and the profiles, the following parameters were estimated: the central meridian of the substorm, the sign conversion latitude, the longitudinal and latitudinal extent. The central meridian is at ~84°MLON during the first two chosen times and at ~106° MLON at the third time. The sign conversion latitude is in the range 60°-67°MLAT, the latitudinal extent – from 25° to 40°, and the longitudinal extent – from 34° to 70° during the stage of the maximal development of the substorm by the 5 nT limit.

Similar results were obtained in previous investigations of expanded substorms.

In latitudinal direction, after the sign conversion latitude X increases fast to the lower latitudes, reaches a maximum, and after decreases gradually. This confirms our previous results about the behavior of the MPB amplitude from the sign conversion latitude to lower latitudes.

In longitudinal direction, the maximal X variations are observed near the crossing of the zero line by Y, thus confirming that the substorm meridian can be determined by both: the location of the maximal X variation in longitudinal direction and the location of the zero of the Y variations. The latitudinal and longitudinal extent increase during the chosen time interval of the expansion phase of the substorm.

European MPB index was computed as the average of the horizontal power by 16 magnetic stations distributed comparatively evenly in Middle Europe. The obtained onset and maximal MPB index value for the considered substorm are very close to the estimations by other authors.

**Acknowledgements.** The authors are grateful to the creators of the databases OMNI (<http://omniweb.gsfc.nasa.gov>), IMAGE (<http://space.fmi.fi/image/>), INTERMAGNET (<http://intermagnet.org/>), SuperMAG (<http://supermag.jhuapl.edu/>), and the solar wind large-scale phenomena catalog (<http://www.iki.rssi.ru/omni/>) for the opportunity to use them in this work.

This study was supported by the National Science Fund of Bulgaria (NSFB) (project number KII-06-Русия/15) and by the RFBR (project number 20-55-18003Болг\_а).

## References

- [1] S.-I. Akasofu, *Several 'Controversial' Issues on Substorms*. Space Sci. Rev. 113, 1–40 (2004). <https://doi.org/10.1023/B:SPAC.0000042938.57710.fb>
- [2] S.-I. Akasofu, *The development of the auroral substorm*, Planet. Space Sci., 12(4), 273–282 (1964).
- [3] M. I. Pudovkin, O. A. Troshichev, *On the types of current patterns of weak geomagnetic disturbances at the polar caps*, Planet. Space Sci., 20, 1773-1779 (1972).
- [4] E. Nielsen, J. Bamber, Z.-S. Chen, A. Brekke, A. Egeland et al., *Substorm expansion into the polar cap*, Ann. Geophys. 6(5), 559-572 (1988).
- [5] I. V. Despirak, A. A. Lyubchich, H. K. Biernat, A. G. Yahnin, *Poleward expansion of the westward electrojet depending on the solar wind and IMF parameters*, Geomagn. Aeronomy. 48(3), 284–292 (2008).
- [6] Feldstein, Y. L., G. V. Starkov, *Dynamics of auroral belt and geomagnetic disturbances*, Planet. Space Sci., 15(2), 209–229 (1967).
- [7] R. L. McPherron, C. T. Russell, M. Aubry, *Satellite studies of magnetospheric substorms on August 15, 1968, 9: phenomenological model for substorms*, J. Geophys. Res., 78(16), 3131–3149 (1973).
- [8] R.L. McPherron, *Substorm related changes in the geomagnetic tail: the growth phase*, Planet. Space Sci., 20(9), 1521-1539 (1972).
- [9] S. B. Mende, R.D. Sharp, E.G. Shelley, G. Haerendel, E.W. Hones, *Coordinated observations of the magnetosphere: The development of a substorm*, J. Geophys. Res., 77(25), 4682-4699 (1972), DOI: 10.1029/JA077i025p04682
- [10] R.L. McPherron, X. Chu, *The midlatitude positive bay and the MPB index of substorm activity*, Space Sci. Rev., 206, 91-122 (2017), DOI: 10.1007/s11214-016-0316-6.
- [11] G. Rostoker, S.-I. Akasofu, J. Foster, R.A. Greenwald, Y. Camide, K. Kawasaki, A.T.Y. Lui, R.L. McPherron, C.T. Russell, *Magnetospheric substorms – definition and signatures*, J. Geophys. Res., 85(A4), 1663-1668 (1980), DOI: 10.1029/JA085iA04p01663
- [12] V. A. Sergeev, N. A. Tsyganenko, *Magnitosfera Zemli*. Nauka, p.174 (1980), (in Russian).
- [13] C.-I. Meng, S.-I. Akasofu, *A study of polar magnetic substorms*, J. Geophys. Res., 74(16), 4035-4053 (1969).
- [14] C.R. Clauer, R.L. McPherron, *Mapping the local time – universal time development of magnetospheric substorms using midlatitude magnetic observations*, J. Geophys. Res., 79(19), 2811-2820 (1974), DOI: 10.1029/JA079i019p02811.
- [15] N. M. Pothier, D.R. Weimer, W.B. Moore, *Quantitative maps of geomagnetic perturbation vectors during substorm onset and recovery*, J. Geophys. Res. Space Physics, 120, 1197–1214 (2015), doi:10.1002/2014JA020602.
- [16] R. Werner, V. Guineva, A. Atanassov, R. Bojilova, L. Raykova, D. Valev, A. Lubchich, I. Despirak, *Calculation of the horizontal power perturbations of the Earth surface magnetic field*, Proc. of the Thirteenth Workshop “Solar Influences on the Magnetosphere, Ionosphere and Atmosphere”, 159-164 (2021a), DOI: 10.31401/ws.2021.proc.
- [17] R. Werner, V. Guineva, A. Lubchich, I. Despirak, R. Bojilova, D. Valev, A. Atanassov, L. Raykova, *Determination of power perturbations of the horizontal magnetic field on the Earth surface*, Proc. Of the Seventeenth International Scientific Conference Space, Ecology, Safety, 34-38 (2021b).
- [18] V. Guineva, R. Werner, I. Despirak, R. Bojilova, L. Raykova, *Mid-latitude positive bays during substorms by quiet and disturbed conditions*, C. R. Acad. Bulg. Sci., 74(8), 1185-1193 (2021a), DOI: 10.7546/CRABS.2021.08.10

- [19] V. Guineva, I. Despirak, R. Werner, R. Bojilova, L. Raykova, *Mid-latitude effects of “expanded” geomagnetic substorms: a case study*, EPJ Web of Conferences, 254, 01004 (2021b), DOI: <https://doi.org/0.1051/epiconf/202125401004>
- [20] P.T. Newell, J.W. Gjerloev, *Evaluation of SuperMAG auroral electrojet indices as indicators of substorms and auroral power*, J. Geophys. Res., 116, A12211 (2011), doi: 10.1029/2011JA016779
- [21] X. Chu, R.L. McPherron, T.-S. Hsu, V. Angelopoulos, *Solar cycle dependence of substorm occurrence and duration: implication for onset*, J. Geophys. Res.: Space Physics, 120, 2808-2818 (2015). <https://doi.org/10.1002/2015ja021104>